One–sided fluid–structure–acoustic coupling for the flow over a flexible structure

Matthias Springer[1], Christoph Scheit[2], Stefan Becker[2]

[1] *Lehrstuhl für Prozessmaschinen und Anlagentechnik, 91058 Erlangen, Deutschland, Email: sp@ipat.uni-erlangen.de*

[2] *Lehrstuhl für Prozessmaschinen und Anlagentechnik, 91058 Erlangen, Deutschland*

Introduction

Sound radiation of technical relevant flows is very often composed of flow and structural noise. Considering technical applications such as cars or planes, as well as cooling devices like fans, flow noise origins from turbulent flow fields, whereas structural noise is generated by oscillating structures. The present work deals with the aeroacoustic sound radiated by a forward–backward facing step in combination with a flexible wall behind the step. Previous numerical and experimental investigations for such a case can be found in Schäfer et al.[1]. In the actual work, a numerical flow computation with coupled aeroacoustic and vibroacoustic simulation was carried out. The structural deformations of the oscillating platelike structure in the wake of the forward–backward facing step are considered to be small and therefore not affecting the flow field. This approach enables a separate consideration for the aeroacoustic as well as the structural borne noise. Additional to the simulations, aeroacoustic measurements in an acoustic wind tunnel were performed for validation purposes.

Numerical Setup

The three–dimensional flow field generated by a forward–backward facing step (Fig. 1) was computed by means of large eddy simulation (LES). The step height H as well as

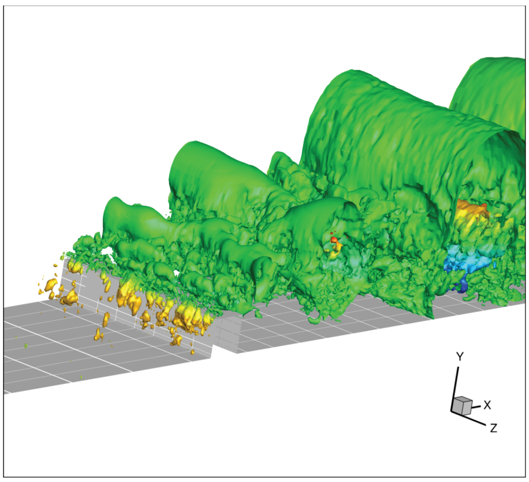

Abbildung 1: Iso–surfaces of pressure fluctuation

the step length was 20 mm. The height of the computational domain was 20H. A symmetry boundary condition was used at the top boundary of the domain. The spanwise extent of the geometry was 10H. In spanwise direction, periodic boundary conditions were applied. At the inflow boundary, a laminar boundary layer profile was set. The velocity at the boundary layer edge was 20 m/s. This yields a Reynolds number of 26.000, based on inflow velocity and step height H. The grid size was chosen to get a wall normal resolution of $y^+ < 1$. The streamwise and spanwise resolution in the wake region of the step was $x^+ < 40$ and $z^+ < 20$, respectively. The overall number of control volumes was 91.6 Millions. The flow computation was carried out using the software FASTEST-3D [2]. This code solves the transient incompressible Navier–Stokes equations. The equations are discretised using the finite volume method (FVM). The influence of the unresolved flow scales was modeled with a Smagorinsky subgrid scale model.

Acoustic source terms were computed within FASTEST-3D based on the flow solution. The present work considered the source term of Lighthill's acoustic analogy. The aeroacoustic sound radiation was computed with the software CFS++ [3] based on the acoustic source terms. This solver uses the finite element method (FEM). The step geometry does not vary in spanwise direction, therefore the aeroacoustic computation was carried out in 2D. The 3D acoustic source terms were averaged over the spanwise direction and conservatively interpolated on the 2D computational aeroacoustic grid. The height of the acoustic domain is 1.05 m. It is surrounded by a perfectly matched layer (PML [4]) to prevent reflections of the sound waves at the boundaries of the domain.

The vibroacoustic sound radiation was based on the surface velocity of the flexible wall right behind the forward–backward facing step. The spanwise and streamwise ex-

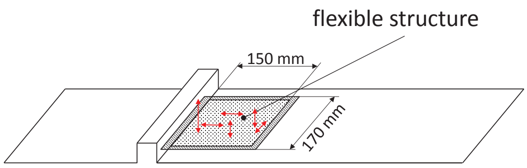

Abbildung 2: Flexible geometry

tension of the plate amounts to 170 mm × 170 mm. The plate was joined on a rigid baffle over a length of 10 mm at the four edges by fixing the corresponding nodes of the mechanical grid. This resulted in an effective flexible area of 150 mm × 150 mm. The plate was modeled as an aluminium plate with a thickness of 3 mm, a density of 2700 kg/m^3 and a modulus of elasticity of $\mathrm{E} = 70 \cdot 10^9 \mathrm{N/m}^2$. The transient surface forces resulted from pressure distribution and wall shear stresses. Based on these forces, the vibration of the plate was computed with CFS++. The propagation of the aeroacoustic sound was computed with the linear wave equation for the acoustic potential Φ:

$$\frac{1}{c^2}\frac{\partial^2\Phi}{\partial t^2} - \frac{\partial^2\Phi}{\partial {x_i}^2} = 0 \tag{1}$$

At the interface between the flexible surface and the acoustic medium, the normal component of the acoustic particle velocity v_i' is equal to the normal component of the mechanical surface velocity v_i^s:

$$n_i v_i' = n_i v_i^s \tag{2}$$

The surface normal vector is donated by n_i. With $v_i' = \frac{\partial \Phi}{x_i}$ the relation between the acoustic potential and the surface velocity is:

$$n_i \frac{\partial \Phi}{x_i} = n_i v_i^s \tag{3}$$

The influence of the surface deformation on the flow field was neglected due to small displacements.

Results

Figure 3 shows the acoustic pressure field generated by the turbulent flow field. Aeroacoustic sound is mainly generated by the shear layer of the recirculation zone in the wake of the step. In Fig. 4, the comparison between the numerical and the experimental results is obvious. The measurements were carried out in the acoustic wind tunnel of the University Erlangen–Nuremberg under anechoic chamber conditions. The numerical and experimental results are compared for a microphone point located 1 m above the step geometry. To compare the results of the 2D aeroacoustic simulation, a sound pressure correction from 2D to 3D had to be performed. According to [5] the relation between the 3D–corrected sound pressure level $SPL_{3D,\Delta}$ radiated by a slice of the width of the step geometry ($\Delta = 10H$) and the sound pressure level of the 2D aeroacoustic simulation SPL_{2D} is:

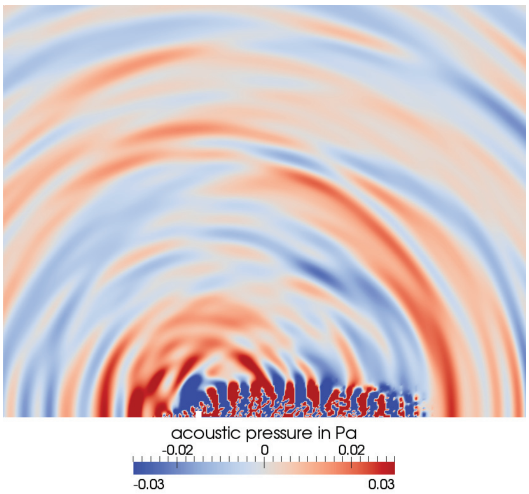

Abbildung 3: Aeroacoustic pressure distribution for an arbitrary time step

$$SPL_{3D,\Delta} = SPL_{2D} + 10\log\left(\frac{f\Delta^2}{Rc_0}\right) \tag{4}$$

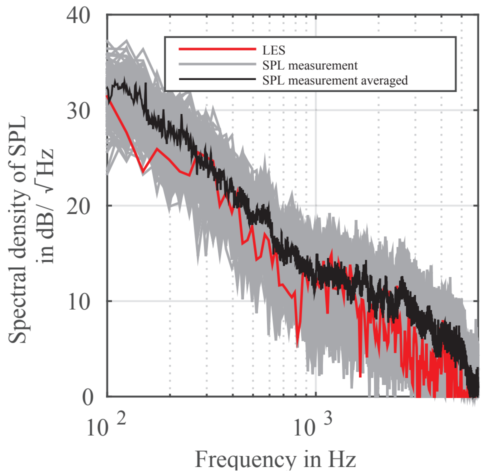

Abbildung 4: Comparison between aeroacoustic measurement and aeroacoustic simulation

The distance to the microphone point is donated by R and the speed of sound by c_0. To compare with the results of the windtunnel measurements, where a nozzle of the width $L = 0.2496$ m was used, an additional correction has to be performed:

$$SPL_{3D,L} = SPL_{3D,\Delta} + 10\log\left(\frac{L}{\Delta}\right) \tag{5}$$

The simulated aeroacoustic results including the corrections of equations (4) and (5) show very good agreement with the measured spectrum. Only minor deviations below the measured results are visible for frequencies below 200 Hz and above 1500 Hz. Additional to the averaged measurements, a superposition of the measured data equally evaluated to the simulated data is shown. The variations of simulated data are located within variations of the superposition of the measured data.

The vibroacoustic sound radiation is driven by the eigenmodes of the flexible plate. The first five computed eigenfrequencies are shown in Table 1. The spectrum of the computed vibroacoustic sound pressure level at a microphone point located 1 m above the step geometry is compared with spectrum of the plate displacement in Figure 5. The comparison with the spectral plate velocity indicates that the vibroacoustic sound radiation is dominated by the eigenmodes of the flexible plate. The SPL of the first eigenmode is 57 dB. The distribution of the vibroacoustic pressure is illustrated in Figure 6.

Tabelle 1: First five computed eigenfrequencies in Hz

1st	2nd	3rd	4th	5th
1160	2359	3469	4209	4232

Conclusion

The present work illustrates a method for the computation of the noise radiated by applications with turbulence as well as structural borne noise. The method enables

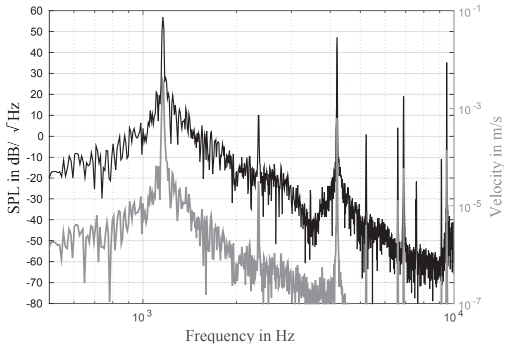

Abbildung 5: Vibroacoustic SPL in comparison with spectrum of mechanical displacement

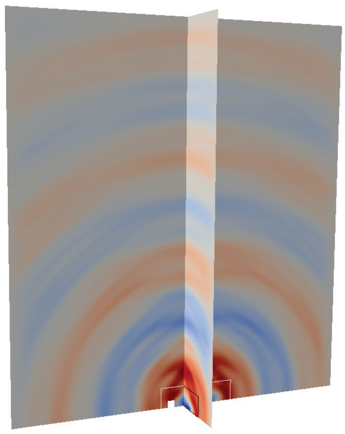

Abbildung 6: Vibroacoustic pressure distribution for an arbitrary time step

a separate consideration of the two mechanisms of noise generation. This is an advantage in comparison to measurements. Due to the detailed computation of the physical field values, insight into the physical mechanisms is enabled. The source term distribution for aeroacoustic sound radiation is able to show regions of enhanced sound generation. The vibroacoustic analysis detects the eigenmodes which dominate the vibration induced sound radiation. The aeroacoustic sound radiation is compared with measurements and shows very good agreement.

Literatur

[1] Schäfer F., Müller, S., Uffinger, T., Becker, S., Grabinger, J.: Fluid–Structure–Acoustics Interaction of the Flow Past a Thin Flexible Structure, *AIAA Journal.*, **48**, (2010).

[2] Durst, F., Schäfer, F. : A Parallel Block/Structured Multigrid Method for the Prediction of Incompressible Flows, *International Journal of Numerical Methods in Fluids*, **22**, 249–565, (1996).

[3] Kaltenbacher, M.: Advanced simulation tool for the design of sensors and actuators. *Procedia Engineering* **5**, 597-600 (2010)

[4] Hüppe, A.: Spectral Finite Elements for Acoustic Field Computation, Dissertation, Vienna University of Technology, (2012)

[5] Oberei, A.A., Roknaldin, F. and Hughes, T.J.R.: Tailing–Edge Noise Due to Turbulent Flows, Report No. 02–002, Boston University, (2002)